Receptor-mediated endocytosis of soluble and membrane-tethered Sonic hedgehog by Patched-1

John P. Incardona*, Ju Ho Lee*, Christie P. Robertson*, Kristi Enga*, Raj P. Kapur†, and Henk Roelink*‡

*Department of Biological Structure and Center for Developmental Biology and †Department of Pathology, University of Washington, Seattle, WA 98195

Edited by Kai Simons, European Molecular Biology Laboratory, Heidelberg, Germany, and approved August 29, 2000 (received for review June 1, 2000)

Patched (Ptc) is the ligand-binding component of the Hedgehog (Hh) receptor complex. In the *Drosophila* embryo, Ptc and Hh colocalize in vesicular punctate structures. However, receptor-mediated endocytosis of Hh proteins has not been demonstrated. By using chick neural plate explants, we show that Sonic hedgehog (Shh)-responsive neural precursor cells internalize recombinant and endogenous Shh and provide direct evidence for a gradient of endogenous Shh in the ventral neural tube. Shh internalization is blocked by a monoclonal antibody whose epitope overlaps the Ptc-binding site of Shh. These findings suggest that Shh internalization is mediated by Ptc-1 and may be linked to signaling. Concordantly, transfection of mammalian cell lines with a Ptc-1 cDNA confers the ability to internalize multiple forms of Shh, including transmembrane-anchored Shh, by a dynamin-dependent process.

Hedgehog (Hh) proteins are extracellular signaling molecules involved in embryonic patterning and organogenesis (1). In vertebrates, Sonic hedgehog (Shh) is essential for dorsal-ventral patterning of the neural tube (2), and explant cultures of neural plate provide one of the best Shh bioassays. In the prevailing model of Hh signal transduction, Patched (Ptc) and Smoothened (Smo) form a receptor complex and act as ligand-binding and signaling subunits, respectively (3). In *Drosophila*, Hh-responsive cells within several cell diameters of Hh-source cells accumulate Ptc and Hh together in punctate structures (4, 5). A relationship of endocytosis to the distribution of Ptc and Hh was shown for each independently by using the *Drosophila shibire*^{ts} (*shi*^{ts}) allele (6, 7), which encodes a temperature-sensitive (ts) dynamin mutant that blocks endocytosis. Ptc was found on endocytic vesicles but accumulated at the plasma membrane when endocytosis was blocked at nonpermissive temperature (7). The subcellular distributions of vertebrate Ptc family members, Ptc-1 and Ptc-2, have not been described, and no study has formally addressed a role for Ptc in receptor-mediated internalization of Hh proteins.

In this study we report that Shh internalization is a normal feature of Shh signaling in neural plate explants that is prevented by antibodies that block binding of Shh to Ptc-1. Cultured mammalian cells do not internalize Shh unless transfected with a Ptc-1 construct, and Shh internalization is blocked by a temperature-sensitive dynamin mutant that disrupts receptor-mediated endocytosis. We also find that cells expressing Ptc-1 can internalize membrane-bound forms of Shh from adjacent cells, including glycosylphosphatidylinositol (GPI)- and transmembrane peptide-anchored Shh fusion proteins. Ptc-mediated removal of diverse forms of Shh from the membranes of adjacent cells is a novel aspect of Ptc function that may be related to the mechanism of Shh signal transduction.

Materials and Methods

Plasmids. Hemagglutinin (HA)-tagged chicken Ptc-1 coding sequence was obtained from pRD67 (8) and subcloned into pMT21 (pMTPtcHA) for expression in mammalian cells. To generate ShhGPI, the mouse *ShhN* cDNA was fused to the sequence encoding the C-terminal GPI signal peptide from decay accelerating factor (9) by using a PCR-based strategy, and subcloned into pBK-cytomegalovirus (CMV) (pBKShhGPI). A sequence encoding the Flag epitope followed by a stop codon was fused in-frame to the C-terminal cytoplasmic tail of ShhCD4 by using a PCR-based strategy. The resulting *ShhCD4F* was subcloned into pRK5 for expression in mammalian cells. Constructs expressing mouse ShhN (pShhN), full-length rat Shh (pMTShh), and mouse ShhCD4 fusion (pcDNA3ShhCD4) have been described (10–12).

Shh Internalization Assays. ShhN was prepared and titrated as described (13). For antibody-blocking experiments, ShhN (1 nM) was incubated for 30 min with 50 μg/ml 5E1 hybridoma supernatant or 50 μg/ml 1D4B supernatant, which recognizes mouse lysosome-associated membrane protein-1 (14); antibody concentrations were estimated by Western blot. Chick neural plate explants were prepared as described (13, 15). Ventral explants with an established floor plate were obtained from the same segment as intermediate explants, whereas ventral explants with a floor plate were obtained from a more anterior region. Explants were cultured with or without 1 nM ShhN for 6 or 12–14 h. Texas Red-conjugated dextran (1–2 mg/ml; Molecular Probes) was added after 6 h of incubation and was continued for 8 h or added at the beginning of a 6- or 12-h incubation. Leupeptin (Sigma; prepared as 0.5-M stock in ethanol) was added at 0.5 mM or ethanol solvent at 0.1% as control. At the end of incubation, explants were washed in PBS, fixed in paraformaldehyde, and processed for Shh, HNF3β, and Pax6 immunofluorescence.

COS-1, COS-7, KNRK, and MDCK cells (all from American Type Culture Collection) were transfected with PtcHA or Shh constructs by using Lipofectamine (GIBCO/BRL). Forty-eight hours after transfection, cells were trypsinized and plated onto poly(D-lysine)-coated coverslips. Some *PtcHA*-transfected cells were incubated for 30 min to overnight with 1 nM ShhN, or for 2 h with 1 mg/ml Texas Red-conjugated dextran in the presence or absence of 1 nM ShhN. KNRK cells expressing PtcHA were cultured with the H^+/ATPase inhibitor concanamycin A (100 nM; Calbiochem) for 1 h before the addition of 1 nM ShhN for 4 h. The effect of concanamycin A was documented by failure to transfer internalized Shh from transferrin-containing endo-

This paper was submitted directly (Track II) to the PNAS office.

Abbreviations: Hh, hedgehog; GPI, glycosyl-phosphatidylinositol; NPC1, Niemann-Pick C1 protein; PIPLC, phosphatidylinositol-specific phospholipase C; Ptc, Patched; Shh, Sonic hedgehog; HA, hemagglutinin; ts, temperature-sensitive; wt, wild type.

‡To whom reprint requests should be addressed at: Department of Biological Structure, University of Washington, 1959 Northeast Pacific Street, Box 357420, HSB G514, Seattle, WA 98195. E-mail: roelink@u.washington.edu.

The publication costs of this article were defrayed in part by page charge payment. This article must therefore be hereby marked "*advertisement*" in accordance with 18 U.S.C. §1734 solely to indicate this fact.

Article published online before print: *Proc. Natl. Acad. Sci. USA*, 10.1073/pnas.220251997. Article and publication date are at www.pnas.org/cgi/doi/10.1073/pnas.220251997

somes to compartments positive for late endosome/lysosome markers. For COS cell cocultures, either *PtcHA*-transfected cells were plated first and then *Shh*-transfected cells were plated on top; or *PtcHA*-transfected cells were mixed with *Shh*-transfected cells and plated simultaneously. As a control, untransfected KNRK cells were cocultured with *Shh*-transfected COS cells; the former were readily distinguished from transfected cells by morphology. Cocultures were incubated at 37°C, washed in PBS and fixed in 4% paraformaldehyde at time points ranging from 2–16 h after plating. Three hours after plating, some samples were transferred from 37°C to room temperature for 30 min, followed by 1 h at 4°C, then subsequently washed and fixed.

HeLa cells stably expressing wild-type (wt) and ts-dynamin under tetracycline control have been described (16). Cells were maintained in medium with 1 μg/ml tetracycline to repress dynamin expression. To induce dynamin overexpression, cells were plated at low density in tetracycline-free medium, which was changed daily for 4 days. Cells were transfected with pMTptcHA by using Lipofectamine on day 2, trypsinized, and seeded onto poly(D-lysine)-coated coverslips on day 3, and assayed for ShhN endocytosis on day 4. To assess transferrin endocytosis, duplicate coverslips were placed in serum-free medium containing 2% BSA for 1 h to deplete transferrin stores. ShhN (1 nM) or Texas Red-conjugated human transferrin (5 μg/ml; Molecular Probes) were then added to cells expressing either dynamin form at 32°C, and after 15 min at 39°C. Cells were incubated at both temperatures for 2 h and then washed, fixed, and processed for PtcHA and Shh immunofluorescence.

Biochemical and Functional Characterization of ShhGPI. COS-1 or 293T cells were transfected with either pBKShhGPI, pMTShh, or pShhN by using Lipofectamine. Sixty hours after transfection, cells were lysed in 20 mM Tris (pH 7.4), 150 mM NaCl, 5 mM EDTA, 1 μg/ml each leupeptin and pepstatin, and either 1% Triton X-100, 1% Triton X-114, or 60 mM *n*-octyl glucoside. Membrane and raft association of ShhGPI, wtShh, and ShhN were compared by differential extraction in cold Triton X-100 and *n*-octyl glucoside, and Triton X-114 partitioning (17). The presence of the GPI was assessed by cleavage with *Bacillus thuringensis* phosphatidylinositol-specific phospholipase C (PIPLC), followed by Triton X-114 partitioning (17). Detergent extracts and samples of medium from transfected cells were assessed by Western blot and detection with polyclonal rabbit anti-Shh. Fusion of the decay accelerating factor C terminus to ShhN converted Shh immunoreactivity from hydrophilic to amphiphilic and membrane-associated, as indicated by shift of the protein from culture medium to the detergent phase of Triton X-114 (data not shown). ShhGPI was partially sensitive to PIPLC cleavage and had extraction properties nearly identical to wtShh: insoluble in cold Triton X-100, but soluble in warm Triton X-100 and cold *n*-octyl glucoside (data not shown). The properties of ShhGPI were essentially identical when expressed in COS-1 or 293T cells. ShhGPI produced Pax7 repression in chick neural plate explants that were cultured on COS-1 or KNRK cells transfected with pShhGPI (data not shown).

Immunofluorescence. Cells were permeabilized and blocked in PBS + 0.1% Triton X-100 + 5% normal goat serum for 30 min at room temperature, then incubated in primary and secondary antibodies diluted in blocking solution each for 1 h at room temperature. Explants embedded in collagen gels were similarly stained, although primary and secondary antibodies were incubated overnight at 4°C, and extensive washes were performed 6–10 h at room temperature. After final washing in PBS, coverslips and explants were mounted in 50% glycerol with phenylenediamine in 0.1 M sodium carbonate (pH 9.5). The following antibodies were used: affinity-purified anti-Shh rabbit polyclonal (S. Morton, H. R., and T. M. Jessell, unpublished results) at 1:500–1:2,000; anti-Shh mAb 5E1 at 1:20; anti-HNF3β mAb 6C7 at 1:20; anti-Pax6 mAb at 1:20 (all from the Developmental Studies Hybridoma Bank, Iowa City, IA); fluorescein-conjugated anti-HA mAb 12CA5 (Boehringer Mannheim) at 1:50 or rat mAb anti-HA (Boehringer Mannheim) at 1:250; fluorescein-conjugated anti-CD4 mAb at 1:100; and biotinylated mouse anti-Flag mAb (Sigma) at 1:250. Secondary antibodies (Jackson ImmunoResearch) were Texas Red- or fluorescein-conjugated donkey-anti-rabbit IgG, Texas Red- or fluorescein-conjugated donkey-anti-rat IgG, all at 1:200; Cy3-conjugated goat-anti-mouse Fab fragment at 1:500; and Cy3-conjugated streptavidin (Zymed) at 1:500. For HNF3β/5E1 double labeling, 2% BSA was used as a blocking agent, and explants were incubated in 5E1, followed by unconjugated goat-anti-mouse Fab fragment at 5 μg/ml, then Texas Red-conjugated donkey-anti-goat IgG; after extensive washing, explants were incubated in anti-HNF3β mAb 6C7, followed by fluorescein-conjugated donkey-anti-mouse IgG.

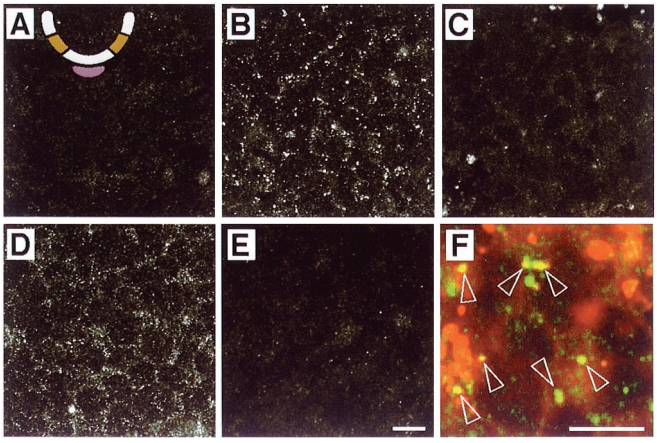

Fig. 1. Internalization of ShhN by neural plate cells in intermediate explants. The intermediate region is ochre and the notochord is mauve in the schematic cross section of the developing neural tube in *A*. Optical sections from the centers of explants are shown. (*A*) Explant incubated without ShhN and stained with polyclonal anti-Shh. (*B*) Explant incubated in 1 nM ShhN for 14 h and stained with polyclonal anti-Shh. (*C*) Explant incubated in 1 nM ShhN for 14 h and stained with anti-Shh mAb 5E1. (*D*) Explant incubated for 14 h in 1 nM ShhN preabsorbed with a mAb 1D4B and stained with polyclonal anti-Shh. (*E*) Explant incubated for 14 h in 1 nM ShhN preabsorbed with anti-Shh mAb 5E1 and stained with polyclonal anti-Shh. (*F*) Explant incubated for 12 h with 1 nM ShhN plus Texas Red-conjugated dextran (red) and stained with polyclonal anti-Shh (green). Open arrowheads highlight Shh$^+$/dextran$^+$ vesicles. The nature of the larger dextran$^+$ structures is unclear. Both scale bars = 10 μm; the bar in *E* applies to *A–D* as well.

Results

Shh Is Internalized by Neural Plate Cells During Signaling. Several lines of evidence indicate that Ptc-1 is the relevant vertebrate Ptc-family member expressed in the neural plate (18–20). To further characterize the cellular aspects of Shh signaling, we examined the distribution of ShhN in neural plate cells in a typical signaling assay. Using affinity-purified polyclonal anti-Shh antibodies, we found that ShhN could be detected in punctate subcellular structures in cells within intermediate explants after overnight (Fig. 1*A* and *B*) or 6-h (data not shown) incubation. Addition of fluorescent dextran, an endocytic tracer, to the culture medium showed that some of these Shh$^+$ structures were endocytic vesicles (Fig. 1*F*). ShhN internalization preceded the stage at which high levels of *Ptc-1* expression are induced by Shh in equivalent regions of the neural tube *in ovo* (18), indicating that ShhN internalization occurs in neural plate

cells expressing low levels of Ptc-1 and is not secondary to high levels of Ptc-1 induced by ShhN.

To assess whether Shh internalization is mediated by Ptc-1, ShhN was preincubated with mAb 5E1, which blocks Shh signaling (21, 22) by preventing binding of Shh to Ptc-1 (23, 24). The epitope recognized by 5E1 appears to overlap the Ptc binding site of ShhN (23, 24). The antibody prevented ShhN internalization (Fig. 1*E*), indicating that ShhN is not internalized simply by nonspecific bulk endocytosis. An irrelevant mAb had no effect on ShhN endocytosis (Fig. 1*D*). Sequential labeling of cells expressing either transfected or endogenous Shh with 5E1 followed by polyclonal anti-Shh showed that bound 5E1 did not prevent detection of Shh by the polyclonal antibody (data not shown). Moreover, internalized ShhN was immunolabeled only with polyclonal Shh antibodies (Fig. 1*B*) and not detected readily with 5E1 (Fig. 1*C*), as expected if the vesicles contain Shh/Ptc complexes in which the 5E1 epitope is masked. Two lines of evidence thus suggest that ShhN endocytosis in neural plate cells requires binding to Ptc-1: internalization is blocked by an antibody whose epitope overlaps the Ptc-1 binding site and consequently prevents binding to Ptc-1, and, once internalized, ShhN cannot be detected with this same antibody.

Naive neural plate cells are first exposed to endogenous cholesterol-modified Shh from the notochord, which induces midline neural plate cells to become Shh-expressing floor plate cells. We thus determined whether neural plate cells adjacent to either the floor plate or notochord internalized Shh derived from either source. Using polyclonal anti-Shh, we observed punctate accumulations of Shh in neural plate cells in an apparent gradient extending more than 10 cell diameters away from Shh source cells in the floor plate (Fig. 2*A*). This gradient of Shh immunoreactivity is superimposed inversely on the graded expression of Pax6 along the dorsoventral axis (Fig. 2*B*). Cells closer to the floor plate with lower Pax6 expression have greater Shh accumulation than more distant cells with higher Pax6 expression. The presence of Shh within Pax6$^+$ cells strongly supports the hypothesis that Shh acts directly on neural precursors in a graded manner to determine cell fate in the ventral neural tube (10, 25). Endogenous Shh$^+$ vesicles were readily detected by polyclonal anti-Shh within cells far from Shh-expressing floor plate cells (Fig. 2 *A* and *B*), but mAb 5E1 detected Shh immunoreactivity predominantly within floor plate cells (Fig. 2*C*), probably in biosynthetic vesicles. This finding is consistent with the masking of the 5E1 epitope in endogenous Shh/Ptc complexes, because, at this stage of development, *Ptc-1* is expressed in a ventral-dorsal gradient with highest levels adjacent to Shh-expressing floor plate cells. Finally, incubation of explants in fluorescent dextran confirmed that ventral neural plate cells accumulate floor plate- or notochord-derived Shh in an endocytic compartment (data not shown and Fig. 2*D*). Addition of leupeptin, a lysosomal protease inhibitor, to the culture medium resulted in an increase in the size and number of dextran$^+$/Shh$^+$ vesicles (Fig. 2*D*), suggesting that internalized Shh is targeted to lysosomes for degradation.

Ptc-1 Confers the Ability to Internalize ShhN by Dynamin-Dependent Endocytosis. Because reagents are not available to study endogenous Ptc-1 in neural plate cells, we characterized potential Ptc-mediated Shh endocytosis by expressing epitope-tagged Ptc-1 (PtcHA) in a variety of mammalian cell lines. When expressed in mammalian cell lines, including COS, HeLa (Fig. 3), MDCK, and KNRK (see supplementary Figs. 5–7, which are published as supplemental data on the PNAS web site, www.pnas.org), PtcHA is found predominantly in intracellular vesicles, with virtually none detectable on the plasma membrane by immunofluorescence. Incubation of *PtcHA*-transfected cells with the same concentration of ShhN used for neural plate cells resulted in the appearance of internalized ShhN within PtcHA$^+$ vesicles (Fig. 3), whereas untransfected cells showed no evidence of Shh uptake (see supplemental Figs. 5–7). As observed for neural plate cells, ShhN internalization was blocked by preincubation with 5E1 (Fig. 3*B*), but not with an irrelevant antibody (Fig. 3*A*). Furthermore, internalized ShhN was detected throughout the cells with polyclonal anti-Shh (Fig. 3*C*), but detected only in a small number of vesicles with 5E1 (Fig. 3*D*), which might suggest that ShhN and Ptc may dissociate at some point along the endocytic pathway, thus exposing the 5E1 epitope. When PtcHA-expressing cells were treated with concanamycin A to block acidification of endosomes (26), 5E1 still detected only a small fraction of the internalized ShhN visible with polyclonal anti-Shh (data not shown). Therefore, the inability to detect internalized Shh with 5E1 is not due to loss of the epitope in the acidic endosomal environment. PtcHA$^+$ vesicles filled with fluorescent dextran to about the same degree in the absence (Fig. 3*E*) or presence of ShhN (Fig. 3*F*), suggesting that Ptc either undergoes a constitutive endocytic cycle or is

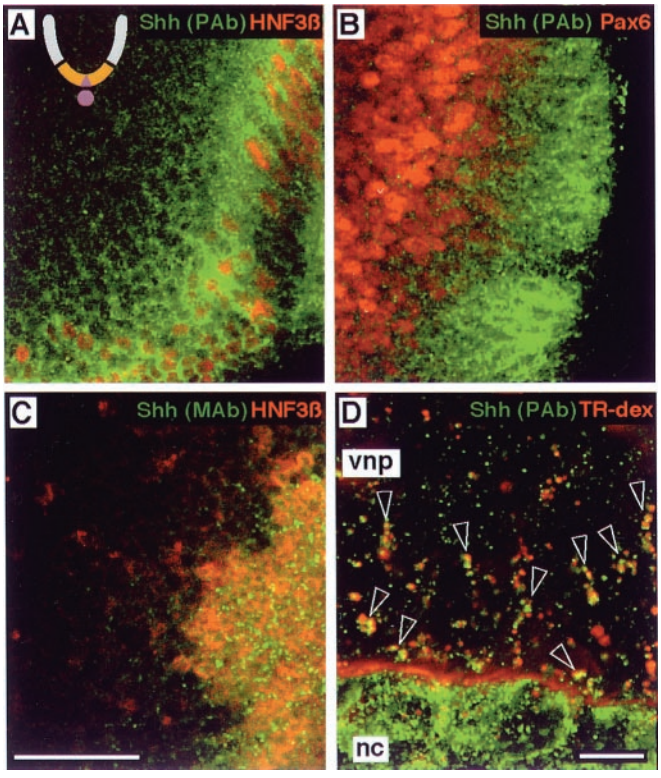

Fig. 2. Ventral neural plate cells internalize endogenous Shh. The ventral region is ochre, and the notochord and floor plate are mauve in the schematic cross section of the developing neural tube in *A*. (*A–C*) Optical sagittal sections with the floor plate to the right/lower right. (*A*) Explant double-labeled with polyclonal anti-Shh (green) and anti-HNF3β (red). The nuclei of HNF3β^+ floor plate cells (red) are evident along the rostral-caudal axis. (*B*) Explant double-labeled with polyclonal anti-Shh (green) and anti-Pax6 (red). Nuclei of cells expressing low levels of Pax6 are immediately adjacent to Pax6-negative floor plate cells, and are surrounded by punctate Shh$^+$ structures. (*C*) Explant double-labeled with anti-Shh mAb 5E1 (green) and anti-HNF3β (red). 5E1 detects punctate structures among HNF3β^+ floor plate nuclei, presumably in secretory vesicles, with scant labeling of HNF3β-negative cells outside the floor plate. (*D*) An explant of ventral neural plate (vnp) with the notochord (nc) attached, from a stage before Shh expression in the floor plate, incubated with 0.5 mM leupeptin and Texas Red-conjugated dextran (red) for 6 h, then stained with polyclonal anti-Shh (green). Dextran is seen within the extracellular space between the notochord and neural plate. Open arrowheads indicate clusters of Shh$^+$/dextran$^+$ endocytic vesicles. Note that Shh$^+$ structures in the notochord do not label with dextran, consistent with a biosynthetic character. Scale bars: 25 μm (*A–C*) and 10 μm (*D*).

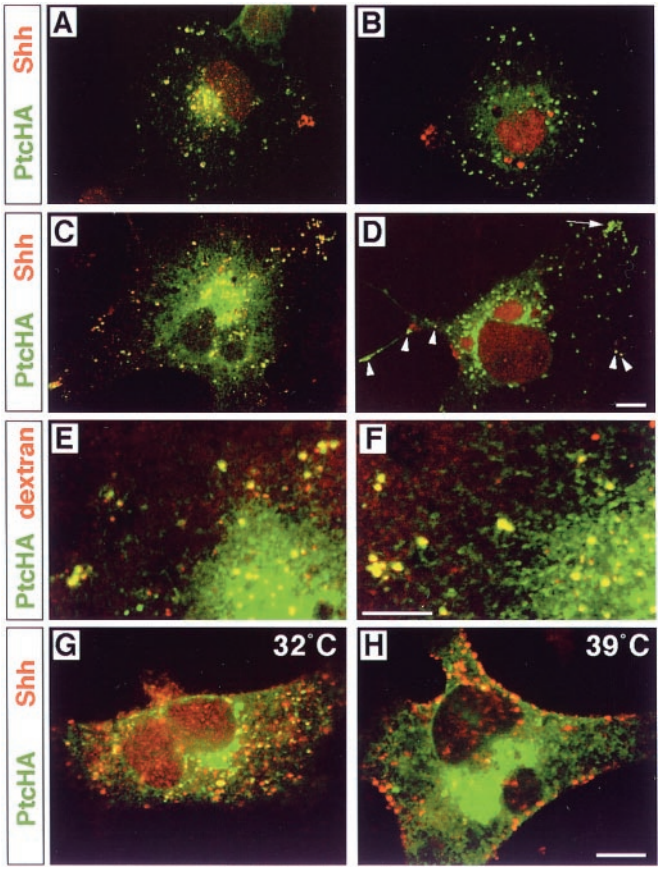

Fig. 3. Requirement of 5E1-sensitive ligand binding and dynamin activity for Ptc-mediated internalization of ShhN and ligand-independent localization of Ptc in endocytic vesicles. PtcHA immunofluorescence is shown in green and Shh immunofluorescence in red; yellow/orange indicates colocalization. (*A*) A single PtcHA-expressing COS cell is shown, incubated for 2 h in 1 nM ShhN pretreated with 50 μg/ml mAb 1D4B. (*B*) A PtcHA-expressing COS cell incubated for 2 h with 1 nM ShhN pretreated with 50 μg/ml (≈275 nM) anti-Shh mAb 5E1. No ShhN is internalized. Some red autofluorescent granules are near the nucleus, as well as debris at the left margin of the cell. (*C*) A single PtcHA-expressing COS cell is shown, incubated in 1 nM ShhN for two hrs, followed by detection with polyclonal anti-Shh. (*D*) A PtcHA-expressing cell incubated in 1 nM ShhN for two hrs, followed by detection with 5E1. Internalized ShhN is detected strongly as yellow signal in only a few isolated vesicles (arrowheads), and weakly in several within a cluster (arrow). Large red autofluorescent granules are near the nucleus. (*E*) A PtcHA-expressing COS cell incubated for 2 h in fluorescent dextran (red). PtcHA$^+$/dextran$^+$ vesicles (yellow) are evident in filopodia as well as the perinuclear region. (*F*) A PtcHA-expressing cell incubated in both 1 nM ShhN and fluorescent dextran for 2 h. PtcHA$^+$/dextran$^+$ vesicles (yellow) are evident in a pattern similar to that in *E*. (*G*) A HeLa cell overexpressing dynamin^{ts} incubated in 1 nM ShhN for 2 h at 32°C. Note that PtcHA$^+$ vesicles with internalized ShhN appear throughout the cytoplasm. (*H*) A PtcHA$^+$ HeLa cell overexpressing dynamin^{ts} incubated in 1 nM ShhN for 2 h starting 15 min after a shift to 39°C. Shh immunofluorescence appears predominantly in large collections at the cell surface. Scale bars = 10 μm (bar in *D* applies to *A–C*; bar in *F* applies to *E*; and bar in *H* applies to *G*).

delivered to an endosomal compartment before reaching the cell surface.

Published results obtained with *shi*^{ts} *Drosophila* embryos suggest that Ptc is rapidly removed from the plasma membrane by dynamin-dependent endocytosis (7). We examined ShhN internalization in *PtcHA*-transfected HeLa cells that stably overexpress temperature-sensitive mutant human dynamin-1 (16) (dynamin^{ts}) containing the analogous mutation as *shi*^{ts} (27) (Fig. 3 *G* and *H*). HeLa cells overexpressing wt dynamin-1 and transfected with *PtcHA* showed normal accumulation of ShhN in PtcHA$^+$ vesicles when cultured at either 32°C or 39°C (see supplementary Figs. 5–7 at www.pnas.org). Similarly, cells overexpressing dynamin^{ts} and transfected with *PtcHA* accumulated ShhN within PtcHA$^+$ vesicles when incubated at permissive temperature (32°C) (Fig. 3*G*). In contrast, when ShhN was added to dynamin^{ts}-expressing cells at nonpermissive temperature (39°C), ShhN immunoreactivity accumulated near the cell surface (Fig. 3*H*), and PtcHA immunoreactivity was more diffuse and appeared to be at or just beneath the plasma membrane in vertical optical sections (see supplementary Figs. 5–7 at www.pnas.org). Receptor-mediated endocytosis of transferrin, assessed in parallel *PtcHA*-transfected cultures, was unaffected in cells overexpressing wt dynamin-1 at either temperature or dynamin^{ts} at 32°C, and blocked in cells overexpressing dynamin^{ts} at 39°C (data not shown). Because HeLa cells expressing dynamin^{ts} restore normal levels of non-clathrin-mediated, fluid-phase bulk endocytosis within 30 min at nonpermissive temperature (16), these findings demonstrate that Shh internalization does not occur through a possible enhancement of bulk endocytosis induced by PtcHA overexpression.

Ptc-1 Mediates the Intercellular Transfer and Endocytosis of Membrane-Bound Forms of Shh. Wild-type Hh proteins are modified by cholesterol at the C terminus (28), and Shh can have palmitate attached to the N terminus (29). These modifications result in the association of Hh with cholesterol-sphingolipid raft membranes (30). Despite the lipid modifications, Hh proteins act several cell diameters away from cells that synthesize them. Chimeric transmembrane forms of Shh (ShhCD4) (12) or *Drosophila* Hh (31) retain signaling activity, as does a GPI-anchored form of *Drosophila* Hh (4), but generally over a shorter range, probably as a consequence of tighter association with source cells. We constructed a GPI-anchored form of Shh (ShhGPI) that was found to be active in the neural plate explant assay (data not shown; see *Materials and Methods*). Although the studies above show that cholesterol-modified wtShh can be internalized, it might be expected that ShhGPI and ShhCD4 would not. We tested the interactions of Ptc-1 with wtShh, ShhGPI, and ShhCD4 by coculturing PtcHA-expressing cells with cells independently transfected with the corresponding *Shh* constructs.

When a cell expressing PtcHA was in contact with a cell expressing wtShh, numerous PtcHA$^+$/Shh$^+$ vesicles were observed (Fig. 4*A*). In addition, PtcHA$^+$/Shh$^+$ vesicles were often observed in PtcHA-expressing cells that were not in direct contact with a wtShh-expressing cell (Fig. 4*B*). Possible explanations for this result include the release of lipid-modified Shh from cells, transient contacts between Shh- and PtcHA-expressing cells before substrate adherence, or the presence of cellular extensions on COS cells analogous to cytonemes (32) that are not observed with our fixation and immunodetection methods but make contact with distant cells.

PtcHA was not detected on the plasma membrane at points of contact between the wtShh- and PtcHA-expressing cells (Fig. 4*A*), even when multiple focal planes were examined (data not shown). This finding suggested that Ptc internalizes wtShh during a brief interaction on the plasma membrane at contact points. To prevent rapid endocytosis, we incubated PtcHA/wtShh cocultures at 25°, then at 4°C. Under these conditions, PtcHA and Shh immunoreactivity were now found to colocalize at points of contact (Fig. 4*C*), indicating that Ptc binds Shh while at the cell surface, and that an active, rapid internalization is responsible for Shh uptake.

When PtcHA-expressing cells contacted ShhGPI-expressing cells, PtcHA$^+$/Shh$^+$ vesicles were observed (Fig. 4*D*). Like wtShh, ShhGPI/PtcHA complexes rapidly entered the endocytic pathway, because PtcHA appeared infrequently at plasma mem-

CELL BIOLOGY

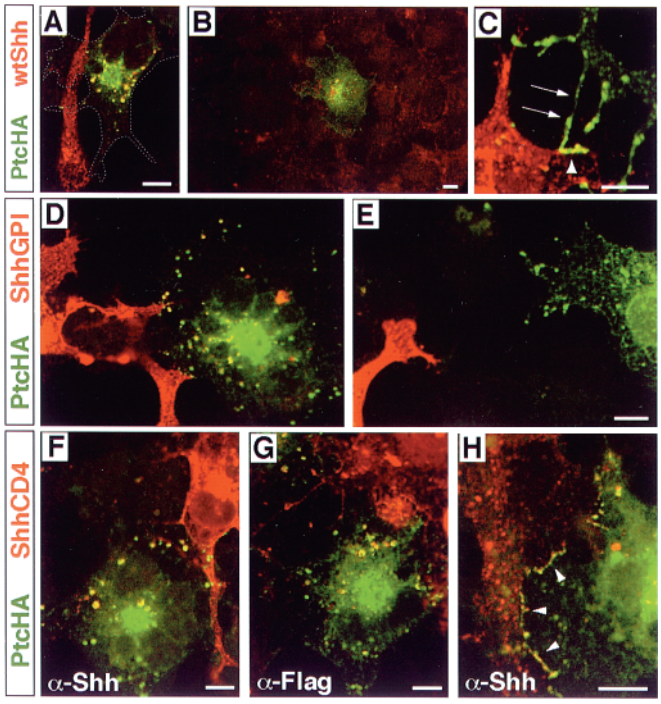

Fig. 4. Internalization of membrane-bound forms of Shh. Throughout, the Shh form is visualized in red and PtcHA in green; colocalization is seen as yellow. (*A*) A PtcHA-expressing cell, whose borders are indicated by the dashed line, is shown contacting a wtShh-expressing cell. PtcHA immunofluorescence is not observed where the filopodium of the wtShh-expressing cell crosses the PtcHA-expressing cell, yet the cell contains multiple $PtcHA^+/Shh^+$ vesicles. (*B*) A PtcHA-expressing cell not in contact with wtShh-expressing cells shows $Shh^+/PtcHA^+$ vesicles. The $PtcHA^+$ cell is surrounded by untransfected cells in a near-confluent field; the nearest wtShh-expressing cell is out of the field of view. Nonspecific background stippling and autofluorescence is evident in untransfected cells. (*C*) PtcHA immunoreactivity colocalizing with wtShh at points of contact between cells at 4°C. Processes of a PtcHA-expressing cell (arrows) are shown contacting a filopodium (arrowheads) of a wtShh-expressing cell. Thirty-three cell pairs were analyzed, which included 10 pairs that were not in direct contact; all showed evidence of Shh internalization. (*D*) A PtcHA-expressing cell is shown in contact with filopodia of two ShhGPI-expressing cells (lower left). $Shh^+/PtcHA^+$ vesicles are yellow. (*E*) Shh immunoreactivity is not observed within a $PtcHA^+$ cell that is in close proximity, but not in contact with a filopodium of a ShhGPI-expressing cell. For ShhGPI, 24 cell pairs in contact were analyzed and all showed evidence of ShhGPI internalization. (*F*) A PtcHA-expressing cell is shown in contact with a ShhCD4-expressing cell (upper right). $Shh^+/PtcHA^+$ vesicles are yellow. (*G*) Two PtcHA-expressing cells are shown in contact with a cell expressing ShhCD4F (upper right), which contains a cytoplasmic Flag epitope. $Flag^+/PtcHA^+$ vesicles are yellow. (*H*) Colocalization of PtcHA and ShhCD4 at points of contact (arrowheads) between cells was observed frequently in cells incubated at 37°C. For ShhCD4, a total of 32 cell pairs in contact were analyzed, and all showed evidence of ShhCD4 internalization. In control experiments, untransfected KNRK cells showed no evidence of Shh internalization when cocultured with COS cells expressing any of the Shh forms. Scale bars = 10 μm (the bar in E applies to D as well).

brane contact points. GPI cleavage is an unlikely explanation for Ptc-mediated uptake. First, a large fraction of ShhGPI expressed in COS cells was resistant to cleavage by PIPLC (data not shown). Second, if COS cells possessed a significant GPI-cleaving activity, then we might expect to find soluble Shh internalized by PtcHA-expressing cells that are not in contact with ShhGPI-expressing cells. In contrast to wtShh, Shh immunoreactivity did not appear in PtcHA-expressing cells that were not in contact with ShhGPI-expressing cells (Fig. 4*E*). These observations suggest either that the GPI anchor possesses a stronger bilayer association than the normal lipid modifications of wtShh, or the cholesterol modification of wtShh is required for some process allowing its release from cells, as has been observed for *Drosophila* Hh (4). Nevertheless, receptor-mediated transendocytosis of a GPI-anchored ligand is unusual.

When PtcHA-expressing cells contacted cells expressing transmembrane-anchored ShhCD4, $PtcHA^+/Shh^+$ vesicles were found within the PtcHA-expressing cells (Fig. 4*F*). The ShhCD4 fusion protein also crossreacts with antibodies against the CD4 ectodomain. The observation of $CD4^+/PtcHA^+$ vesicles (data not shown) suggests that the entire ShhCD4 molecule is transferred into PtcHA-expressing cells. To rule out proteolytic cleavage proximal to the transmembrane segment, we generated a ShhCD4 construct with a Flag epitope on the cytoplasmic tail (ShhCD4F). When PtcHA-expressing cells were cultured in contact with ShhCD4F-expressing cells, $Flag^+/PtcHA^+$ vesicles were observed (Fig. 4*G*), indicating that the entire ShhCD4F molecule had been internalized. PtcHA-expressing cells that were not in contact with ShhCD4-expressing cells showed no Shh, CD4, or Flag immunoreactivity (data not shown). In contrast to both wtShh and ShhGPI, PtcHA was often found at multiple contact points in association with ShhCD4 on adjacent cells cultured at 37°C (Fig. 4*H*). Examination of multiple focal planes often showed extensive cell-surface colocalization, with small, apparently interdigitated membrane structures on neighboring $PtcHA^+$ and ShhCD4 $^+$ cells (see supplemental Figs. 5–7 at www.pnas.org). These findings suggest that the endocytosis of ShhCD4 is delayed considerably relative to the forms that are anchored only in the outer leaflet and further confirms that, under normal circumstances, Ptc moves rapidly between an intracellular compartment and the cell surface. These findings indicate that internalization of Shh is a very prominent function of Ptc-1.

Discussion

Our findings indicate that receptor-mediated endocytosis of Shh is an inherent activity of Ptc-1 and that Shh internalization is a feature of signaling in neural plate cells. However, in contrast to many cell-surface receptors, Ptc-1 is not detected at significant levels on the cell surface at steady state. Instead, when overexpressed in many cell types, Ptc-1 is found mainly on a population of endosomal vesicles, and it can be visualized at the cell surface only by blocking or significantly delaying its internalization. Disruption of dynamin function blocks Shh internalization, suggesting classical receptor-mediated endocytosis via clathrin-coated pits. However, the finding of Ptc-1 in $dextran^+$ vesicles in the absence of Shh suggests that Ptc-1 has constitutive, ligand-independent internalization signals, which may account for its steady-state endosomal distribution. The unusual ability for Ptc-1 to retrieve membrane-bound Shh forms from adjacent cells indicates that removal of Shh from the extracellular milieu is a prominent feature of Ptc function, and it is possible that internalization of Shh may be linked to signal transduction.

In *Drosophila*, endogenous Ptc protein is most readily detected in cells that have already responded to Hh and have up-regulated Ptc expression; in these cells, Ptc and Hh immunoreactivity colocalize strongly in vesicles. The gradient of internalized Shh near the floor plate probably reflects a similar situation, because a gradient of increased *Ptc* transcription is apparent adjacent to the floor plate after its formation (18). *Ptc-1* transcripts are initially expressed in neuroepithelium below the level of detection but are dramatically up-regulated in response to Shh signaling (18–20), suggesting that protein levels also would be very low initially. However, our results with intermediate region explants indicate that internalization of Shh is an early aspect of Shh signaling in naive neural plate cells, suggesting that even low levels of Ptc rapidly remove Shh from the cell surface.

Receptor-mediated endocytosis of transmembrane ligands is uncommon, but is well documented for two receptor systems in

Drosophila and *Caenorhabditis elegans*. The Sevenless receptor tyrosine kinase mediates the internalization of the polytopic ligand Boss in developing photoreceptors (33), and Notch homologues can mediate the internalization of their transmembrane Delta and Serrate ligands (34–36). In each case, the mechanism of uptake is not known. However, some studies have suggested that the mechanism is not phagocytic, but may involve transfer of small patches of membrane along with the ligand, or extraction of the ligands without transfer of significant amounts of membrane lipid components (35, 37). Although none of these receptor/ligand complexes have been localized to clathrin-coated pits, double membrane-containing coated pits were observed during endocytosis of a transmembrane-anchored cell adhesion molecule at sites of homophilic interactions between *Aplysia* neurons (38).

We suspect that the avid internalization of Shh by Ptc-1 could reflect its relationship to the Niemann-Pick C1 (NPC1) protein (39, 40), and may have implications for NPC1 function. Although the precise function of NPC1 is unknown, it is found on endosomal vesicles, and appears to be involved in the retrieval and redistribution of cholesterol and associated lipids derived from the endocytic pathway (41). NPC1 and Ptc may use similar mechanisms to transfer their respective cargo between membrane-bound compartments. The Ptc/NPC1 relationship deserves further study, especially in light of the sensitivity of both NPC1 function and Shh signal transduction to many of the same pharmacologic agents (42). The actions of these drugs suggest that Ptc-mediated Shh internalization and signal transduction may be linked.

We thank Cliff Tabin for providing the *PtcHA* cDNA, Sandra Schmid for the HeLa cells expressing wt and mutant dynamin; Han Huang for the DAF C terminus construct, Andy McMahon for the ShhCD4 fusion construct, Andy Farr for the anti-CD4 antibody, Terry Rosenberry for purified PIPLC, and Susan Morton and Tom Jessell for the affinity-purified anti-Shh antibodies. J.H.L. was a Howard Hughes Medical Institute summer undergraduate fellow. This work was supported by grants from the National Institute on Environmental Health Sciences (ES09210) to H.R. and R.P.K. and to the University of Washington Center for Ecogenetics and Environmental Health (ES07033); and a McKnight Endowment Fund for Neuroscience Scholar Award to H.R.

1. Hammerschmidt, M., Brook, A. & McMahon, A. P. (1997) *Trends Genet.* **13,** 14–21.
2. Briscoe, J. & Ericson, J. (1999) *Semin. Cell Dev. Biol.* **10,** 353–362.
3. Murone, M., Rosenthal, A. & de Sauvage, F. J. (1999) *Exp. Cell Res.* **253,** 25–33.
4. Burke, R., Nellen, D., Bellotto, M., Hafen, E., Senti, K.-A., Dickson, B. J. & Basler, K. (1999) *Cell* **99,** 803–815.
5. Bellaiche, Y., The, I. & Perrimon, N. (1998) *Nature (London)* **394,** 85–88.
6. Tabata, T. & Kornberg, T. B. (1994) *Cell* **76,** 89–102.
7. Capdevila, J., Pariente, F., Sampedro, J., Alonso, J. L. & Guerrero, I. (1994) *Development* **120,** 987–998.
8. Marigo, V., Davey, R. A., Zuo, Y., Cunningham, J. M. & Tabin, C. J. (1996) *Nature (London)* **384,** 176–179.
9. Huang, J.-H., Getty, R. R., Chisari, F. V., Fowler, P., Greenspan, N. S. & Tykocinski, M. L. (1994) *Immunity* **1,** 607–613.
10. Roelink, H., Porter, J. A., Chiang, C., Tanabe, Y., Chang, D. T., Beachy, P. A. & Jessell, T. M. (1995) *Cell* **81,** 445–455.
11. Roelink, H., Augsburger, A., Heemskerk, J., Korzh, V., Norlin, S., Ruiz i Altaba, A., Tanabe, Y., Placzek, M., Edlund, T., Jessell, T. M., *et al*. (1994) *Cell* **76,** 761–775.
12. Yang, Y., Drossopoulou, G., Chuang, P. T., Duprez, D., Marti, E., Bumcrot, D., Vargesson, N., Clarke, J., Niswander, L., McMahon, A., *et al*. (1997) *Development* **124,** 4393–4404.
13. Incardona, J. P., Gaffield, W., Lange, Y., Cooney, A., Pentchev, P. G., Liu, S., Watson, J. A., Kapur, R. P. & Roelink, H. (2000) *Dev. Biol.* **224,** 440–452.
14. Chen, J. W., Pan, W., D'Souza, M. P. & August, J. T. (1985) *Arch. Biochem. Biophys.* **239,** 574–586.
15. Incardona, J. P., Gaffield, W., Kapur, R. P. & Roelink, H. (1998) *Development* **125,** 3553–3562.
16. Damke, H., Baba, T., van der Bliek, A. M. & Schmid, S. L. (1995) *J. Cell Biol.* **131,** 69–80.
17. Incardona, J. P. & Rosenberry, T. L. (1996) *Mol. Biol. Cell* **7,** 595–611.
18. Marigo, V. & Tabin, C. J. (1996) *Proc. Natl. Acad. Sci. USA* **93,** 9346–9351.
19. Goodrich, L. V., Johnson, R. L., Milenkovic, L., McMahon, J. A. & Scott, M. P. (1996) *Genes Dev.* **10,** 301–312.
20. Goodrich, L. V., Milenkovic, L., Higgins, K. M. & Scott, M. P. (1997) *Science* **277,** 1109–1113.
21. Ericson, J., Morton, S., Kawakami, A., Roelink, H. & Jessell, T. M. (1996) *Cell* **87,** 661–673.
22. Pagan-Westphal, S. M. & Tabin, C. J. (1998) *Cell* **93,** 25–35.
23. Fuse, N., Maiti, T., Wang, B., Porter, J. A., Hall, T. M., Leahy, D. J. & Beachy, P. A. (1999) *Proc. Natl. Acad. Sci. USA* **96,** 10992–10999.
24. Pepinsky, R. B., Rayhorn, P., Day, E. S., Dergay, A., Williams, K. P., Galdes, A., Taylor, F. R., Boriack-Sjodin, P. A. & Garber, E. A. (2000) *J. Biol. Chem.* **275,** 10995–11001.
25. Ericson, J., Rashbass, P., Schedl, A., Brenner Morton, S., Kawakami, A., van Heyningen, V., Jessell, T. M. & Briscoe, J. (1997) *Cell* **90,** 169–180.
26. Drose, S. & Altendorf, K. (1997) *J. Exp. Biol.* **200,** 1–8.
27. van der Bliek, A. M. & Meyerowitz, E. M. (1991) *Nature (London)* **351,** 411–414.
28. Porter, J. A., Young, K. E. & Beachy, P. A. (1996) *Science* **274,** 255–259.
29. Pepinsky, R. B., Zeng, C., Wen, D., Rayhorn, P., Baker, D. P., Williams, K. P., Bixler, S. A., Ambrose, C. M., Garber, E. A., Miatkowski, K., *et al*. (1998) *J. Biol. Chem.* **273,** 14037–14045.
30. Rietveld, A., Neutz, S., Simons, K. & Eaton, S. (1999) *J. Biol. Chem.* **274,** 12049–12054.
31. Strigini, M. & Cohen, S. M. (1997) *Development* **124,** 4697–4705.
32. Ramirez-Weber, F. A. & Kornberg, T. B. (1999) *Cell* **97,** 599–607.
33. Cagan, R. L., Kramer, H., Hart, A. C. & Zipursky, S. L. (1992) *Cell* **69,** 393–399.
34. Henderson, S. T., Gao, D., Lambie, E. J. & Kimble, J. (1994) *Development* **120,** 2913–2924.
35. Klueg, K. M., Parody, T. R. & Muskavitch, M. A. (1998) *Mol. Biol. Cell* **9,** 1709–1723.
36. Klueg, K. M. & Muskavitch, M. A. (1999) *J. Cell Sci.* **112,** 3289–3297.
37. Sunio, A., Metcalf, A. B. & Kramer, H. (1999) *Mol. Biol. Cell* **10,** 847–859.
38. Bailey, C. H., Chen, M., Keller, F. & Kandel, E. R. (1992) *Science* **256,** 645–649.
39. Carstea, E. D., Morris, J. A., Coleman, K. G., Loftus, S. K., Zhang, D., Cummings, C., Gu, J., Rosenfeld, M. A., Pavan, W. J., Krizman, D. B., *et al*. (1997) *Science* **277,** 228–231.
40. Loftus, S. K., Morris, J. A., Carstea, E. D., Gu, J. Z., Cummings, C., Brown, A., Ellison, J., Ohno, K., Rosenfeld, M. A., Tagle, D. A., *et al*. (1997) *Science* **277,** 232–235.
41. Blanchette-Mackie, E. J. (2000) *Biochim. Biophys. Acta* **1486,** 171–183.
42. Incardona, J. P. & Eaton, S. (2000) *Curr. Opin. Cell Biol.* **12,** 193–203.